

Codon populations in single-stranded whole human genome DNA are fractal and fine-tuned by the Golden Ratio 1.618

Jean-claude Perez φ

Abstract: This new bioinformatics research bridges Genomics and Mathematics. We propose a universal “Fractal Genome Code Law”: **The frequency of each of the 64 codons across the entire human genome is controlled by the codon's position in the Universal Genetic Code table.** We analyze the frequency of distribution of the 64 codons (codon usage) within single-stranded DNA sequences. Concatenating 24 Human chromosomes, we show that the entire human genome employs the well known universal genetic code table as a *macro* structural model. The position of each codon within this table precisely dictates its population. So the Universal Genetic Code Table not only maps codons to amino acids, but serves as a global checksum matrix. Frequencies of the 64 codons in the whole human genome scale are a self-similar fractal expansion of the universal genetic code. The original genetic code kernel governs not only the micro scale but the macro scale as well. Particularly, the 6 folding steps of codon populations modeled by the binary divisions of the “*Dragon fractal paper folding curve*” show evidence of 2 attractors. The numerical relationship between the attractors is derived from the Golden Ratio. We demonstrate that:

1. The whole Human Genome Structure uses the Universal Genetic Code Table as a tuning model. It pre-determines global codons proportions and populations. The Universal Genetic Code Table governs both micro and macro behavior of the genome.
2. We extend the *Chargaff's* second rule from the domain of single TCAG nucleotides to the larger domain of codon triplets.
3. Codon frequencies in the human genome are clustered around 2 fractal-like attractors, strongly linked to the golden ratio 1.618.

Keywords: Interdisciplinary, Bioinformatics, Mathematics, Human Genome decoding, Universal Genetic Code, *Chargaff's* rules, Noncoding DNA, Symmetry, Chaos Theory, Fractals, Golden Ratio, Checksum, Cellular automata, DNA strands atomic weights balance.

1 Introduction

Aside from a few obscure papers, *fractals* and the *golden ratio* have not been considered relevant to DNA or the study of the human genome. However, two major papers in the journal *Science* in October 2009 and January 2010 have stimulated the genetics community to pursue new lines of inquiry within these concepts.

First, in October 2009, in a prominent paper (Lieberman-Aiden *et al.*, 2009), *E. Lieberman-Aiden* used Hi-C mass technology to probe the three-dimensional architecture of the whole genome. They explored the chromatin conformation folding of the whole human genome on a megabase scale. Their research reveals it to be consistent with a fractal globule model.

The cover of *Science Magazine* (Lander, 2009) showed a folding Hilbert fractal curve. Dr. Eric Lander (Science Adviser to the President and Director of the Broad Institute) enthusiastically announced: “**Mr. President, the Genome is Fractal!**”

For the first time, they proved at a physical level, the fractal nature (Mandelbrot, 1953) of human genome DNA molecule, including chromatin (DNA + proteins, i.e. Histones).

“*Since the PHYSICAL structure was found fractal (providing enormous amount of untangled compression), it is reasonable that the LOGICAL sequence and function of the genome are also fractal.*” (Pellionisz, A., 2009, personal communication: From the Principle of Recursive

φ Email: jeanclaudeperez2@free.fr Jean-claude Perez 7 avenue de terre-rouge F33127 Martignas France, 33-0950507849.

Genome Function to Interpretation of HoloGenome Regulation by Personal Genome Computers. Cold Spring Harbor Laboratory. Personal Genomes Conference, Sept. 14-17, 2009).

Secondly, in January 2010, the journal *Science* reported that the golden ratio is present in the atomic scale of the magnetic resonance of spins of cobalt niobate atoms (Coldea *et al.*, 2010). When applying a magnetic field at right angles to an aligned spin, the magnetic chain shifts into a new state called “quantum critical.” New properties emerge from *Heisenberg's* Uncertainty Principle.

For the last 20 years, whole genomes have revealed traces of fractal behavior as various publications studied the logical level of both elementary gene-coding or non-coding TCAG single DNA sequences. In *Nature* in 1992, C.K. Peng found trace evidence of fractals in analyzing DNA sequences (Peng *et al.*, 1992).

Models of fractal integer patterns, like *Fibonacci* or *Lucas* numbers, have been proposed: In 1991 we proposed that Golden Ratio Fibonacci/Lucas integer numbers define strong relationships between DNA gene-coding region sequences and Fibonacci's embedded TCAG gene sequence patterns (Perez, 1991). We also prove the optimality of these patterns (Perez, 1997) in the book *L'ADN décrypté (“Deciphering DNA”)* [@]. Examples involving evolution and pathogen analysis include genes or small genes-rich genomes [§] especially the HIV genome.

Then, in 2007, Yamagishi proposed evidence of *Fibonacci* based organization and verified it at a statistical global level across the whole human genome. (Yamagishi *et al.*, 2008).

For several years, other researchers like A. Pellionisz advocated ways to analyze and detect fractal defects within whole genomes. This is based on recursive fractal exploration methods and artificial neural network technologies (Pellionisz, 2008).

Then finally, simultaneously with the (Lander, 2009) October 2009 paper, we showed in the book ***Codex Biogenesis*** (Perez, 2009) a convergence of evidence for whole genome fractal organization. This comes from analyzing whole genomes not at a physical level, but at the logical level of TCAG single stranded sequenced DNA. These findings were obtained primarily by analyzing the finalized human genome sequence (Baltimore, 2001).

The goal of the present paper is show fractal behavior in the genome at the *logical* DNA analysis level. We provide an exhaustive analysis of codon frequencies on a whole human genome scale.

This analysis classifies the 64 codon populations combined with various embedded foldings of the universal genetic code map. This is based on the DRAGON curve (Gardner, 1967) also called the “folding paper curve” (see figure a). It reveals the fractal structure of the whole human genome at the DNA sequential information scale.

This analysis reveals that codon frequencies are oriented around 2 numerical attractors. The distance separating the attractors is “1/2Phi”, where Phi is the “Golden ratio”. These discoveries simultaneously extend the reach of *Chargaff's* second rule for single-stranded DNA of the whole Human Genome.

[@] This book explores a numerical property called « *DNA Supracode* » consisting of an exhaustive combinatorial research of « *resonances* » within gene-coding DNA sequences: a resonance is an exact Fibonacci/Lucas nucleotide number harmonious proportion. For example: 144 contiguous TCAG nucleotides have exactly 55 T nucleotides and 89 A or C or G nucleotides. Then a resonance exists with an exact Golden ratio proportion as defined in the Methods section: 55, 89 and 144 are consecutive Fibonacci numbers following the Golden Ratio. Gene-rich genomes like HIV have thousands « *resonances* », where the longer ones are overlapping 2/3rds of the whole genome length.

[§] Research on HIV-SIV isolates genomic diversity with the support of Pr *Luc Montagnier*, FMPRS (World Foundation for AIDS research and Prevention (UNESCO), 1 rue Miollis, 75015, Paris, France).

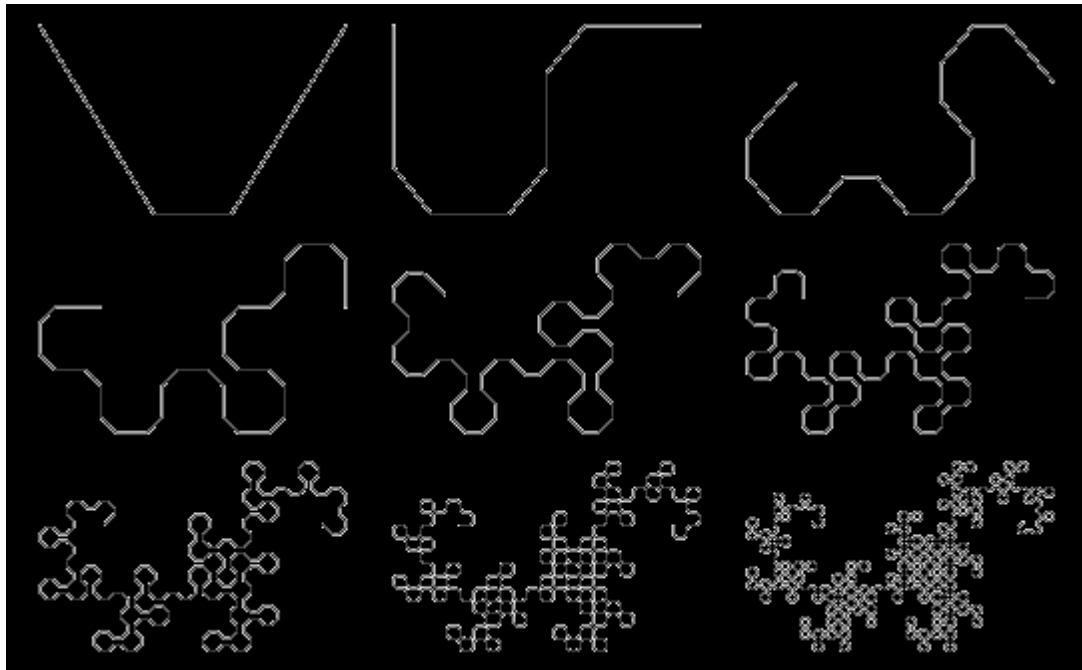


Figure a- The Dragon curve or “paper folding” embedded fractal dynamics.

2 Methods

Human genome release analysed with Dragon curve folding.

We analyzed the entirety of the whole human genome from the 2003 “BUILD34” finalized release #. We considered only the main single strand of the DNA sequence. Within this sequence, we computed, for each of the 3 possible codon reading frames, the cumulative number of each of the 64 genetic code codons &.

This process £ analyzes the sequence of 24 human chromosomes. Then all 64 codon populations are totaled, adding the 3 codon reading frames and the 24 chromosomes. The total count is exactly of 2.843.411.612 codons.

Now the 64 codon populations are arranged according to the 4 columns of the well known Universal Genetic Code map (column T, then column C, then column A, then column G). Then this list is partitioned successively 6 ways according to the 6 binary splits of the dragon curve dynamical folding (see figure b):

Dragon1: 2 partitions of 32 codons each.

Dragon2: 4 partitions of 16 codons each.

Dragon3: 8 partitions of 8 codons each.

Dragon4: 16 partitions of 4 codons each.

Dragon5: 32 partitions of 2 codons each.

Dragon6: 64 partitions of 1 codon each.

Human genome finalized BUILD34. Build 34 finished human genome assembly (hg16, Jul 2003).

<http://hgdownload.cse.ucsc.edu/goldenPath/hg16/chromosomes/>

& The full detailed data relating codon populations for the 3 codon reading frame and for the 24 human chromosomes is available in supplementary materials.

£ Computer language used for this research was the parallel interactive mathematical language APL+WIN (APL language – A Programming Language – invented by K.E. Iverson in 1957 at Harvard University began as a mathematical notation for manipulating arrays that he taught to his students. Then, in 1964, APL was implemented in computers by IBM).

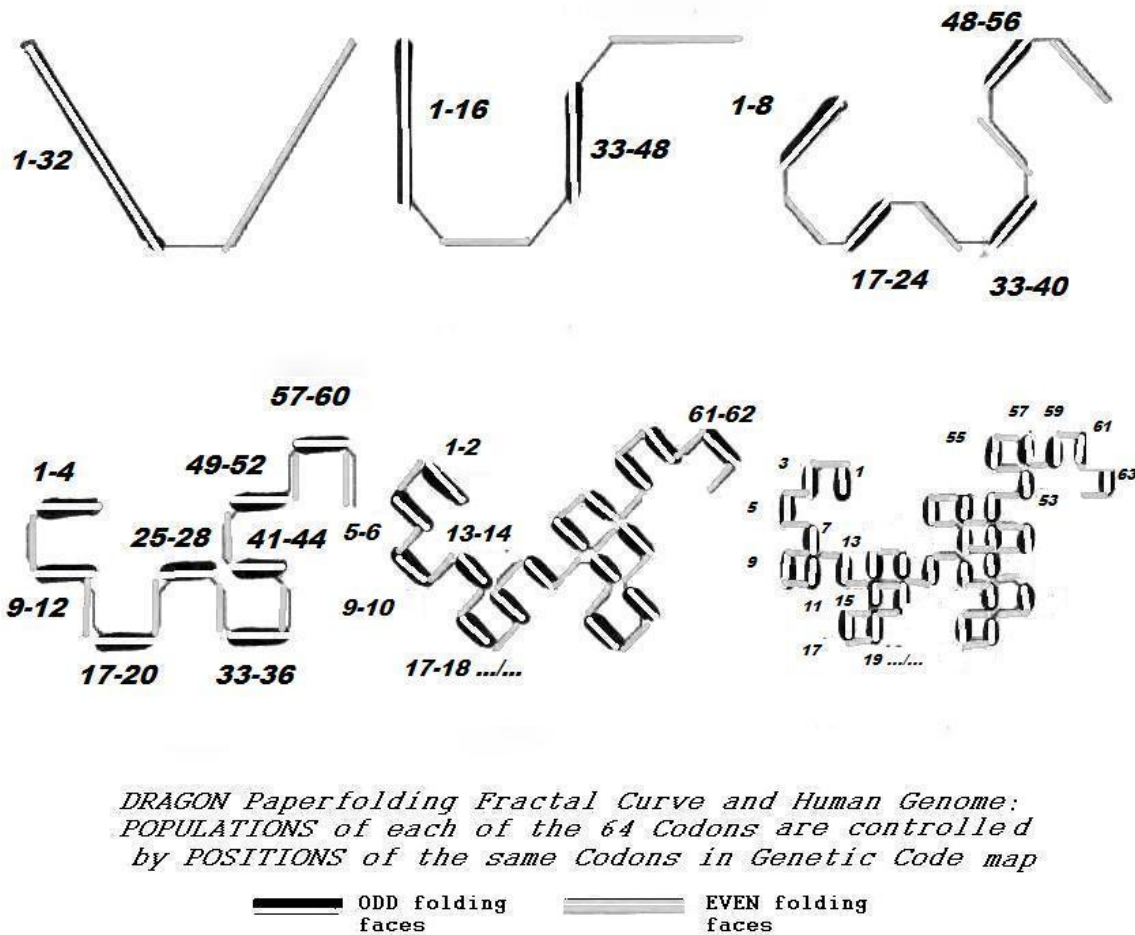


Figure b- Six Dragon curve folds of the whole human genome 64 codon populations.

Golden ratio overview.

“Phi”, the Golden ratio, is an irrational number. Its value is approximately 1.618. It was introduced initially by *Euclid* (Euclid, 1533 first printed Edition). He provides the first known written definition of Phi: *“A straight line is said to have been cut in extreme and mean ratio when, as the whole line is to the greater segment, so is the greater to the less”*.

To summarize: if “a+b” is the whole line, and “a” is the larger segment and “b” is the smaller segment, then:

$$(a + b) / a = a / b = \text{Phi}$$

The numerical value of the Golden ratio is 1.6180339887...

The golden ratio has fascinated people of diverse interests for at least 2,400 years. But in scientific research it's considered more of an intellectual curiosity than a source of rigorous technical insight. Many are unsure of how to apply it.

But it is observed in many major scientific disciplines: for example, in artificial neural networks (Perez, 1990), superconductors (Perez, 1994), and quantum physics:

- Coldea describes his discovery of Golden ratio in quantum Physics at the beginning of his paper (Coldea et al., 2010): *“To analyze these nanoscale quantum effects researchers have chosen the cobalt niobate material consisting of linked magnetic atoms, which form thin chains one atom wide. This model is useful to describe ferromagnetism on the nanoscale in solid matter. Applying a magnetic field on aligned spin from the magnetic chain will transform it into a new matter state called quantum critica, which recalls the quantum version of a fractal pattern. Then, the system reaches a kind of quantum uncertain Schrödinger cat state.”*

Dr. Radu Coldea from Oxford University, who is the principal author of the paper, explains: *"Here the tension comes from the interaction between spins causing them to magnetically resonate. For these interactions we found a series (scale) of resonant notes: The first two notes show a perfect relationship with each other. Their frequencies (pitch) are in the ratio of 1.618..., which is the golden ratio famous in art and architecture."* There is no coincidence. *"It reflects a beautiful property of the quantum system – a hidden symmetry. Actually quite a special one called E8 by mathematicians, and this is its first observation in a material."*

- In other fields, the Golden ratio was also recently discovered within a magnetic compound (Affleck, 2010). The introductory paper abstract is typical in its ambiguous assessment of the Golden Ratio's scientific merit: *"The golden ratio — an exact 'magic' number often claimed to be observed when taking ratios of distances in ancient and modern architecture, sculpture and painting — has been spotted in a magnetic compound."*
- In (Calleman, 2009), the author reports that *« Golden Ratio is also involved in the universal Bohr radius formula measuring a single electron orbits hydrogen's atom nucleus and its smallest possible orbit, with lowest energy, which is the most likely position of the electron ».*

3 Results

Tables 1 through 6 summarize a remarkable phenomenon: The Universal Genetic Code plays the role of a macro-level structural matrix. This matrix controls and balances the exact codon populations within the whole human genome. Results are similar whether the starting point of the codons reading frame sequence is the first, second or third nucleotide. We observe a flip-flop binary balance around 2 attractors: "1" and a single formula based on $\Phi=1.618033$, commonly called the "golden ratio" which controls morphogenesis spirals in nature like pineapples, cactus, nautilus etc.

The distance separating both attractors is $\frac{1}{2} \Phi$. Note that the figure c provides a typical "band-based" mechanism common in *Poincare's* chaos theory. In fact, figure c provides a strong network of $2^6=64$ binary state constraints, establishing the 64 basic codon locations *and* populations.

We suggest a possible explanation, analyzing figure c Dark/Light bands. All ratios based on A or G bands, divided by T or C bands, correspond to attractor « 1 ». Odd-indexed Dragons are dragon1, dragon3 and dragon5 in figure c.

Similarly, all ratios based on C or G bands divided by T or A bands correspond to attractor « $(3-\Phi)/2$ ». Even-indexed Dragons are dragon2, dragon4 dragon6 in figure c.

As summarized in figure c, we can say that ratios between codons sorted by A or G in the second base position (by columns) and codons sorted by T or C in the second base position cluster around **attractor « 1 »**.

Similarly, ratios between codons sorted by C or G in second base position and codons sorted by T or A in second base position cluster around **attractor « $(3-\Phi)/2$ »**.

We can show that both attractors are present in the two other possible vectorizations of genetic code table. In other words, the result is the same whether we start sorting with the first base, second base or third base of codons (by lines, i.e. sorting by the first base of codons; or by columns, i.e. sorting by the second base of codons; or, also, sorting by the third base of codons).

Specifically, the distance between both attractors «1» and « $(3-\Phi)/2$ » is exactly **" $\frac{1}{2}\Phi$ " where $\Phi=1.618\dots$ is the "Golden ratio"**.

The synthesis of the 6 Dark/Light subset patterns in figure c highlights the 64 specific codon populations differentiation constraints. This is the governing checksum matrix.

Now we can reformulate our introductory sentence as follows:

“Populations of each of the 64 codons within whole human genome single-stranded DNA sequence are controlled by the positions of these same codons in the Universal Genetic Code table... and finally by the nucleotide compositions of these elementary codons”.

Results Part I: Total codon populations, adding the 3 codon reading frames for the whole human genome single-stranded DNA sequence.

		SECOND NUCLEOTIDE					
		T	C	A	G		
FIRST NUCLEOTIDE	T	TTT 109591342 2.4667	TCT 62964984 1.4172	TAT 58718182 1.3216	TGT 57468177 1.2935	T	THIRD NUCLEOTIDE
		TTC 56120623 1.2632	TCC 43850042 0.9870	TAC 32272009 0.7264	TGC 40949883 0.9217	C	
		TTA 59263408 1.3339	TCA 55697529 1.2536	TAA 59167883 1.3318	TGA 55709222 1.2539	A	
		TTG 54004116 1.2155	TCG 6265386 0.1410	TAG 36718434 0.8265	TGG 52453369 1.1806	G	
	C	CTT 56828780 1.2791	CCT 50494519 1.1365	CAT 52236743 1.1758	CGT 7137644 0.1607	T	
		CTC 47838959 1.0768	CCC 37290873 0.8393	CAC 42634617 0.9596	CGC 6737724 0.1517	C	
		CTA 36671812 0.8254	CCA 52352507 1.1784	CAA 53776608 1.2104	CGA 6251611 0.1407	A	
		CTG 57598215 1.2964	CCG 7815619 0.1759	CAG 57544367 1.2952	CGG 7815677 0.1759	G	
	A	ATT 71001746 1.5981	ACT 45731927 1.0293	AAT 70880610 1.5954	AGT 45794017 1.0307	T	
		ATC 37952376 0.8542	ACC 33024323 0.7433	AAC 41380831 0.9314	AGC 39724813 0.8941	C	
		ATA 58649060 1.3201	ACA 57234565 1.2882	AAA 109143641 2.4566	AGA 62837294 1.4144	A	
		ATG 52222957 1.1754	ACG 7117535 0.1602	AAG 56701727 1.2763	AGG 50430220 1.1351	G	
	G	GTT 41557671 0.9354	GCT 39746348 0.8946	GAT 37990593 0.8551	GGT 33071650 0.7444	T	
		GTC 26866216 0.6047	GCC 33788267 0.7605	GAC 26820898 0.6037	GGC 33774033 0.7602	C	
		GTA 32292235 0.7268	GCA 40907730 0.9208	GAA 56018645 1.2609	GGA 43853584 0.9871	A	
		GTG 42755364 0.9623	GCG 6744112 0.1518	GAG 47821818 1.0764	GGG 37333942 0.8403	G	

Table 1 - The 64 codon populations of the whole human genome for the 3 codon reading frames of single stranded DNA (2843411612 codons). In this figure, the 3 values in each cell are: the codon label, the codon's total population, the “Codon Frequency Ratio” (CFR). CFR is computed as: codon population x 64 / 2.843.411.612. (where 2.843.411.612 is the whole genome cumulated codons). Then, if CFR < 1, the codon is rare, if CFR>1, the codon is frequent.

Results Part II: Total codon populations for each codon reading frame for the whole human genome single-stranded DNA sequence.

	T	C	A	G	
T	36530115	20990387	19568343	19152113	T
	18708048	14614789	10755607	13649076	C
	19750578	18565027	19721149	18562015	A
	18005020	2087242	12240281	17480496	G
C	18944797	16835177	17423117	2379612	T
	15942742	12428986	14214421	2244432	C
	12217331	17444649	17927956	2085226	A
	19195946	2606672	19176935	2604253	G
A	23669701	15251455	23634011	15266057	T
	12650299	11007307	13794251	13242724	C
	19548709	19073189	36381293	20948987	A
	17409063	2372235	18894716	16810797	G
G	13852086	13252828	12658530	11026602	T
	8955434	11268094	8938833	11258126	C
	10766854	13635427	18678084	14619310	A
	14252868	2247440	15939419	12446600	G

Table 2 – Whole Human Genome total codon populations, reading the single-stranded DNA sequence using the 1st codon reading frame for all 24 chromosomes.

	T	C	A	G	
T	36531484	20990069	19567591	19161459	T
	18705099	14616282	10759233	13642011	C
	19760072	18562218	19721384	18573930	A
	18000027	2087896	12235265	17485497	G
C	18943023	16830651	17407468	2378865	T
	15947740	12434383	14204715	2245855	C
	12231662	17448562	17919791	2083233	A
	19207416	2605584	19186320	2605633	G
A	23665435	15239476	23626173	15260933	T
	12652839	11009466	13794560	13238715	C
	19553135	19080857	36382485	20947165	A
	17412586	2373311	18905269	16804537	G
G	13849120	13246918	12663136	11018601	T
	8958446	11258715	8942549	11261722	C
	10762798	13639976	18670370	14617066	A
	14254024	2248753	15939572	12444755	G

Table 3 – Whole Human Genome total codon populations, reading the single-stranded DNA sequence using the 2nd codon reading frame for all 24 chromosomes.

	T	C	A	G	
T	36529743	20984528	19582248	19154605	T
	18707476	14618971	10757169	13658796	C
	19752758	18570284	19725350	18573277	A
	17999069	2090248	12242888	17487376	G
C	18940960	16828691	17406158	2379167	T
	15948477	12427504	14215481	2247437	C
	12222819	17459296	17928861	2083152	A
	19194853	2603363	19181112	2605791	G
A	23666610	15240996	23620426	15267027	T
	12649238	11007550	13792020	13243374	C
	19547216	19080519	36379863	20941142	A
	17401308	2371989	18901742	16814886	G
G	13856465	13246602	12668927	11026447	T
	8952336	11261458	8939516	11254185	C
	10762583	13632327	18670191	14617208	A
	14248472	2247919	15942827	12442587	G

Table 4 – Whole Human Genome total codon populations reading the single-stranded DNA sequence using the 3rd codon reading frame for all 24 chromosomes.

Results Part III: Paper folding Dragon curve fractals applied 6 times to the Universal Genetic Code table.

		Second Position of Codon				
		T	C	A	G	
T	TTT Phe [F]	TCT Ser [S]	TAT Tyr [Y]	TGT Cys [C]	T C A G	
	TTC Phe [F]	TCC Ser [S]	TAC Tyr [Y]	TGC Cys [C]		
	TTA Leu [L]	TCA Ser [S]	TAA Ter [end]	TGA Ter [end]		
	TTG Leu [L]	TCG Ser [S]	TAG Ter [end]	TGG Trp [W]		
C	CTT Leu [L]	CCT Pro [P]	CAT His [H]	CGT Arg [R]	T C A G	
	CTC Leu [L]	CCC Pro [P]	CAC His [H]	CGC Arg [R]		
	CTA Leu [L]	CCA Pro [P]	CAA Gln [Q]	CGA Arg [R]		
	CTG Leu [L]	CCG Pro [P]	CAG Gln [Q]	CGG Arg [R]		
A	ATT Ile [I]	ACT Thr [T]	AAT Asn [N]	AGT Ser [S]	T C A G	
	ATC Ile [I]	ACC Thr [T]	AAC Asn [N]	AGC Ser [S]		
	ATA Ile [I]	ACA Thr [T]	AAA Lys [K]	AGA Arg [R]		
	ATG Met [M]	ACG Thr [T]	AAG Lys [K]	AGG Arg [R]		
G	GTT Val [V]	GCT Ala [A]	GAT Asp [D]	GGT Gly [G]	T C A G	
	GTC Val [V]	GCC Ala [A]	GAC Asp [D]	GGC Gly [G]		
	GTA Val [V]	GCA Ala [A]	GAA Glu [E]	GGA Gly [G]		
	GTG Val [V]	GCG Ala [A]	GAG Glu [E]	GGG Gly [G]		

1st dragon curve folding
Dragon 1: ratio Dark/Light = 1

		Second Position of Codon				
		T	C	A	G	
T	TTT Phe [F]	TCT Ser [S]	TAT Tyr [Y]	TGT Cys [C]	T C A G	
	TTC Phe [F]	TCC Ser [S]	TAC Tyr [Y]	TGC Cys [C]		
	TTA Leu [L]	TCA Ser [S]	TAA Ter [end]	TGA Ter [end]		
	TTG Leu [L]	TCG Ser [S]	TAG Ter [end]	TGG Trp [W]		
C	CTT Leu [L]	CCT Pro [P]	CAT His [H]	CGT Arg [R]	T C A G	
	CTC Leu [L]	CCC Pro [P]	CAC His [H]	CGC Arg [R]		
	CTA Leu [L]	CCA Pro [P]	CAA Gln [Q]	CGA Arg [R]		
	CTG Leu [L]	CCG Pro [P]	CAG Gln [Q]	CGG Arg [R]		
A	ATT Ile [I]	ACT Thr [T]	AAT Asn [N]	AGT Ser [S]	T C A G	
	ATC Ile [I]	ACC Thr [T]	AAC Asn [N]	AGC Ser [S]		
	ATA Ile [I]	ACA Thr [T]	AAA Lys [K]	AGA Arg [R]		
	ATG Met [M]	ACG Thr [T]	AAG Lys [K]	AGG Arg [R]		
G	GTT Val [V]	GCT Ala [A]	GAT Asp [D]	GGT Gly [G]	T C A G	
	GTC Val [V]	GCC Ala [A]	GAC Asp [D]	GGC Gly [G]		
	GTA Val [V]	GCA Ala [A]	GAA Glu [E]	GGA Gly [G]		
	GTG Val [V]	GCG Ala [A]	GAG Glu [E]	GGG Gly [G]		

2nd dragon curve folding
Dragon 2: ratio Dark/Light = (3 - Phi) / 2

		Second Position of Codon				
		T	C	A	G	
T	TTT Phe [F]	TCT Ser [S]	TAT Tyr [Y]	TGT Cys [C]	T C A G	
	TTC Phe [F]	TCC Ser [S]	TAC Tyr [Y]	TGC Cys [C]		
	TTA Leu [L]	TCA Ser [S]	TAA Ter [end]	TGA Ter [end]		
	TTG Leu [L]	TCG Ser [S]	TAG Ter [end]	TGG Trp [W]		
C	CTT Leu [L]	CCT Pro [P]	CAT His [H]	CGT Arg [R]	T C A G	
	CTC Leu [L]	CCC Pro [P]	CAC His [H]	CGC Arg [R]		
	CTA Leu [L]	CCA Pro [P]	CAA Gln [Q]	CGA Arg [R]		
	CTG Leu [L]	CCG Pro [P]	CAG Gln [Q]	CGG Arg [R]		
A	ATT Ile [I]	ACT Thr [T]	AAT Asn [N]	AGT Ser [S]	T C A G	
	ATC Ile [I]	ACC Thr [T]	AAC Asn [N]	AGC Ser [S]		
	ATA Ile [I]	ACA Thr [T]	AAA Lys [K]	AGA Arg [R]		
	ATG Met [M]	ACG Thr [T]	AAG Lys [K]	AGG Arg [R]		
G	GTT Val [V]	GCT Ala [A]	GAT Asp [D]	GGT Gly [G]	T C A G	
	GTC Val [V]	GCC Ala [A]	GAC Asp [D]	GGC Gly [G]		
	GTA Val [V]	GCA Ala [A]	GAA Glu [E]	GGA Gly [G]		
	GTG Val [V]	GCG Ala [A]	GAG Glu [E]	GGG Gly [G]		

3rd dragon curve folding
Dragon 3: ratio Dark/Light = 1

		Second Position of Codon				
		T	C	A	G	
T	TTT Phe [F]	TCT Ser [S]	TAT Tyr [Y]	TGT Cys [C]	T C A G	
	TTC Phe [F]	TCC Ser [S]	TAC Tyr [Y]	TGC Cys [C]		
	TTA Leu [L]	TCA Ser [S]	TAA Ter [end]	TGA Ter [end]		
	TTG Leu [L]	TCG Ser [S]	TAG Ter [end]	TGG Trp [W]		
C	CTT Leu [L]	CCT Pro [P]	CAT His [H]	CGT Arg [R]	T C A G	
	CTC Leu [L]	CCC Pro [P]	CAC His [H]	CGC Arg [R]		
	CTA Leu [L]	CCA Pro [P]	CAA Gln [Q]	CGA Arg [R]		
	CTG Leu [L]	CCG Pro [P]	CAG Gln [Q]	CGG Arg [R]		
A	ATT Ile [I]	ACT Thr [T]	AAT Asn [N]	AGT Ser [S]	T C A G	
	ATC Ile [I]	ACC Thr [T]	AAC Asn [N]	AGC Ser [S]		
	ATA Ile [I]	ACA Thr [T]	AAA Lys [K]	AGA Arg [R]		
	ATG Met [M]	ACG Thr [T]	AAG Lys [K]	AGG Arg [R]		
G	GTT Val [V]	GCT Ala [A]	GAT Asp [D]	GGT Gly [G]	T C A G	
	GTC Val [V]	GCC Ala [A]	GAC Asp [D]	GGC Gly [G]		
	GTA Val [V]	GCA Ala [A]	GAA Glu [E]	GGA Gly [G]		
	GTG Val [V]	GCG Ala [A]	GAG Glu [E]	GGG Gly [G]		

4th dragon curve folding
Dragon 4: ratio Dark/Light = (3 - Phi) / 2

		Second Position of Codon				
		T	C	A	G	
T	TTT Phe [F]	TCT Ser [S]	TAT Tyr [Y]	TGT Cys [C]	T C A G	
	TTC Phe [F]	TCC Ser [S]	TAC Tyr [Y]	TGC Cys [C]		
	TTA Leu [L]	TCA Ser [S]	TAA Ter [end]	TGA Ter [end]		
	TTG Leu [L]	TCG Ser [S]	TAG Ter [end]	TGG Trp [W]		
C	CTT Leu [L]	CCT Pro [P]	CAT His [H]	CGT Arg [R]	T C A G	
	CTC Leu [L]	CCC Pro [P]	CAC His [H]	CGC Arg [R]		
	CTA Leu [L]	CCA Pro [P]	CAA Gln [Q]	CGA Arg [R]		
	CTG Leu [L]	CCG Pro [P]	CAG Gln [Q]	CGG Arg [R]		
A	ATT Ile [I]	ACT Thr [T]	AAT Asn [N]	AGT Ser [S]	T C A G	
	ATC Ile [I]	ACC Thr [T]	AAC Asn [N]	AGC Ser [S]		
	ATA Ile [I]	ACA Thr [T]	AAA Lys [K]	AGA Arg [R]		
	ATG Met [M]	ACG Thr [T]	AAG Lys [K]	AGG Arg [R]		
G	GTT Val [V]	GCT Ala [A]	GAT Asp [D]	GGT Gly [G]	T C A G	
	GTC Val [V]	GCC Ala [A]	GAC Asp [D]	GGC Gly [G]		
	GTA Val [V]	GCA Ala [A]	GAA Glu [E]	GGA Gly [G]		
	GTG Val [V]	GCG Ala [A]	GAG Glu [E]	GGG Gly [G]		

5th dragon curve folding
Dragon 5: ratio Dark/Light = 1

"1" Attractor: "Odd" Folding

		Second Position of Codon				
		T	C	A	G	
T	TTT Phe [F]	TCT Ser [S]	TAT Tyr [Y]	TGT Cys [C]	T C A G	
	TTC Phe [F]	TCC Ser [S]	TAC Tyr [Y]	TGC Cys [C]		
	TTA Leu [L]	TCA Ser [S]	TAA Ter [end]	TGA Ter [end]		
	TTG Leu [L]	TCG Ser [S]	TAG Ter [end]	TGG Trp [W]		
C	CTT Leu [L]	CCT Pro [P]	CAT His [H]	CGT Arg [R]	T C A G	
	CTC Leu [L]	CCC Pro [P]	CAC His [H]	CGC Arg [R]		
	CTA Leu [L]	CCA Pro [P]	CAA Gln [Q]	CGA Arg [R]		
	CTG Leu [L]	CCG Pro [P]	CAG Gln [Q]	CGG Arg [R]		
A	ATT Ile [I]	ACT Thr [T]	AAT Asn [N]	AGT Ser [S]	T C A G	
	ATC Ile [I]	ACC Thr [T]	AAC Asn [N]	AGC Ser [S]		
	ATA Ile [I]	ACA Thr [T]	AAA Lys [K]	AGA Arg [R]		
	ATG Met [M]	ACG Thr [T]	AAG Lys [K]	AGG Arg [R]		
G	GTT Val [V]	GCT Ala [A]	GAT Asp [D]	GGT Gly [G]	T C A G	
	GTC Val [V]	GCC Ala [A]	GAC Asp [D]	GGC Gly [G]		
	GTA Val [V]	GCA Ala [A]	GAA Glu [E]	GGA Gly [G]		
	GTG Val [V]	GCG Ala [A]	GAG Glu [E]	GGG Gly [G]		

6th dragon curve folding
Dragon 6: ratio Dark/Light = (3 - Phi) / 2

"(3 - Phi) / 2" Attractor: "Even" Folding

Figure c – The 6 fractal-like embedded structure of whole human genome codon populations.

Fractal Embedded Foldings	Total Odd (ODD)	Total Even (EVEN)	Ratios Odd/Even	Ratios Even/Odd	Attractors
DRAGON1	1422241146	1421170466	1.000753379		1
DRAGON2	1681042486	1162369126	1.446220868	0.6914573162	(3-Phi)/2
DRAGON3	1422240864	1421170748	1.000752982		1
DRAGON4	1681042231	1162369381	1.446220331	0.6914575729	(3-Phi)/2
DRAGON5	1422241420	1421170192	1.000753765		1
DRAGON6	1681042267	1162369345	1.446220407	0.6914575367	(3-Phi)/2

Table 5 - Detailed results show the 2 Phi-based fractal attractors.

<p>-I- 2 parts = 2*1 Dragon 1 2x32 Halves</p> <p>The ratio between the EVEN Half part and the ODD half part is</p> <p>= 0.999247 = 1 (error=0.000753)</p>	<p>-II- 4 parts = 4*1 Dragon 2 4x16 Quartiles</p> <p>The ratio between EVEN Quartiles and ODD Quartiles is</p> <p>= 0.691457 = (3 – Phi) / 2 (error=0.000474)</p>	<p>-III- 8 parts = 2*3 Dragon 3 8x8 Octants</p> <p>The ratio between EVEN Octants and ODD Octants is</p> <p>= 0.999248 = 1 (error=0.000752)</p>
<p>-IV- 16 parts = 4*2 Dragon 4 16x4 Squares</p> <p>The ratio between EVEN Squares and ODD Squares is</p> <p>= 0.691458 = (3 – Phi) / 2 (error=0.000475)</p>	<p>-V- 32 parts = 2*5 Dragon 5 32x2 Binomes</p> <p>The ratio between EVEN Binomes and ODD Binomes is</p> <p>= 0.999247 =1 (error=0.000753)</p>	<p>-VI- 64 parts = 4*3 Dragon 6 64x1 codons</p> <p>The ratio between EVEN Codons and ODD Codons is</p> <p>= 0.691458 = (3 – Phi) / 2 (error=0.000474)</p>

Table 6 - Chessboard map summarizing major results, attractors and symmetries.

4 Discussion

Now we ask several questions:

1. "Why does the universal genetic code also serve as a self-similar matrix that determines codon populations across the whole human genome?"
2. "Is this fractal structure universal for all genomes?"
3. "What is its relationship to Chargaff's rules?"
4. "Why isn't the chaos pattern of human genome codons just random chance?"

1. "Why does the universal genetic code also serve as a self-similar matrix that determines codon populations across the whole human genome?"

This is very strange. Everything unfolds as if the populations held concurrently by the 64 codons in the whole human genome scale are a self-similar fractal projection of the original universal genetic code primitive matrix.

A central question is: Is this directly from an ancestral original source or is this the result of ongoing self-regulation and genome process tuning?

We believe this serves as a checksum matrix which ensures that harmful mutations can be regulated and corrected. This is not unlike checksums in computer programs. *Perry Marshall* suggested to me that perhaps it goes further than that, supervising the structure of genome rearrangement and transpositions.

Finally, the big question that remains is: “*How did the human genome structure discover and select natural symmetries from Universal Genetic Code map to use as a checksum mechanism?*” This question takes us to the very frontiers of science!

-2- “Is this fractal structure universal for all genomes?”

We analyzed whole genomes using the same method. From the analysis of about twenty various species like eukaryotes, viruses etc. (Perez, 2009, chapter 19), it appears that:

If we sort the codon populations according to the genetic code table forming 8 clusters of 8 codons each, then: 3 parameters – involved in a cellular automata generation process - define codon populations within these genomes to a precision of 99%, and often 99.999%. These 3 parameters are: the number "1", and two other parameters which are always linked to the Golden ratio Phi. For the human and chimpanzee genomes, codon frequencies are 99.99% correlated. These 3 parameters are “1, 2 and Phi”. We remark that these 3 specific numbers establish a distance of $\frac{1}{2}$ Phi separating both attractors, as discovered in this study.

-3- “What is the relationship to Chargaff's rules?”

This is probably the most interesting relationship we explore in this paper. *Chargaff's* two parity rules are:

- First *Chargaff* parity rule: in double-stranded DNA, %T=%A and %C=%G.
- Second *Chargaff* parity rule (Rudner *et al.*, 1968): in a single-stranded DNA, %T=%A and %C=%G.

Are there links between our discovery of single-stranded whole human genome sequence codon populations and *Chargaff's* rules? One might be tempted to judge that our results are a trivial consequence of *Chargaff's* second rule.

But in reality, these new results extend *Chargaff's* second rule from the simple TCAG nucleotide level to the codon triplet level as well.

In 2006, *Albrecht-Buehler* suggests that *Chargaff's* second rule appears to be the consequence of a more complex parity rule (Albrecht-Buehler, 2006). Combining large quantities of data and checking for triplet oligonucleotides, *Albrecht-Buehler* has suggested that this possible extension of *Chargaff's* second rule to triplet oligonucleotides might be a consequence of genomic evolution, particularly transposon activity.

Computing Chargaff's second rule for the whole human genome nucleotide level.

Using data from tables 2, 3, and 4, it is easy to calculate the amount and percentages of TCAG nucleotides within whole human genome single-stranded DNA. We consider successively the three codon reading frames populations. In these 3 cases we compute the quantities of TCAG nucleotides. Then we check validity and regularity of *Chargaff's* second parity rule at the global scale of whole human genome. Particularly, table 7 demonstrates that the error of *Chargaff's* second parity rule is about 1/1000. Variation from codon reading frame to codon reading frame is infinitesimal (these fluctuations result from undetermined nucleotides regions frontiers from DNA sequencing process). Meanwhile, we note also that $T/A > 1$ and $C/G < 1$. **However, the most remarkable fact is the**

presence of both attractors «(3-Phi)/2» and «1» at the global T C A G nucleotide scale, as computed from line 1 in Table 7. In effect, attractor «1» corresponds to *Chargaff's* second rule T=A and C=G which we have just demonstrated here. The second attractor «(3-Phi)/2» is seen when we compute ratios T/C=1.447808424, A/G=1.444633555 and (T+A)/(C+G)=1.446220557. When you compare these results with those of Table 5, they are extremely close to the ideal value $2 / (3-\Phi) = 1.447213595$.

Verifying Chargaff's second rule within single stranded DNA whole human genome						
	T	C	A	G	T/A	C/G
1 st frame	841214808	581026325	839827524	581342944	1.001651868	0.9994553662
2 nd frame	841214825	581026348	839827527	581342943	1.001651884	0.9994554075
3 rd frame	841214769	581026355	839827531	581342937	1.001651813	0.9994554299

Table 7 – checking for Chargaff's second parity rule at the whole human genome scale.

Towards a codon level generalization of *Chargaff's* second rule.

We can reorganize the 2D data codon populations of the Table 1 into a 3D array of 4x4x4 cells, according to the three TCAG codons positions.

Then we can construct this cubic array for each of the 3 codon positions as follows:

Codon total populations	T codons	C codons	A codons	G codons
3 rd position	841214933	581026487	839827334	581342858
2 nd position	841214880	581026266	839827606	581342860
1 st position	841214589	581026275	839827642	581343106

Table 8 – A Chargaff-like second parity rule is verified at the “codon scale level” analyzing the total codon population of the 3 codon reading frames within the single-stranded whole human genome DNA sequence.

In the first left column, the first cell cumulates codons of type « xyT », the second cell cumulates codons of type « xTy » and the last cell cumulates codons of type « Txy » and so on. The same process applied to only one codon reading frame (i.e. data from Tables 2 or 3 or 4) produces similar results.

Finally we can extend the scope of *Chargaff's* second rule from the single nucleotide TCAG level to the global level of codon triplets.

Now we suggest a new codon-level *Chargaff* second parity rule:

In the whole human genome simple-stranded DNA sequence, Chargaff's second rule can be extended to all triplets codons as follows:

- *Codon populations where first base position is T are identical to codon populations where first base position is A, therefore: « **codons Twx = codons Ayz** ».*
- *Codon populations where first base position is C are identical to codon populations where first base position is G, therefore: « **codons Cwx = codons Gyz** ».*
- *Codon populations where 2nd base position is T are identical to codon populations where second base position is A, therefore: « **codons wTx = codons yAz** ».*
- *Codon populations where 2nd base position is C are identical to codon populations where second base position is G, therefore: « **codons wCx = codons yGz** ».*
- *Codon populations where third base position is T are identical to codon populations*

where third base position is A, therefore: « **codons wxT = chdons yzA** ».

- Codon populations where third base position is C are identical to codon populations where third base position is G, therefore: « **codons wxC = codons yzG** ».

Verifying this law at the level of individual chromosomes in the human genome.

We refer to data in the supplementary materials which shows codon populations for each human chromosome. It is possible to verify the proposed *Chargaff* second rule codon extension at the scale of each individual human chromosome single-stranded DNA sequence. This results emphasize variability in the related law T>A and C<G:

T>A is verified in 18 of 24 chromosomes, but C<G is only verified in 14 of 24 chromosomes. We note also the T=A is highly variable in chromosome Y, probably resulting from the fact that the Y chromosome has a very low instance of chromosome-crossing in evolution.

Computing errors on CODON level Chargaff's 2 nd rule differences T=A and C=G in relative %	1 st codon position T > or = A ratio T/A	2 nd codon position T > or = A ratio T/A	3 rd codon position T > or = A ratio T/A	1 st codon position C < or = G ratio C/G	2 nd codon position C < or = G ratio C/G	3 rd codon position C < or = G ratio C/G
Chromosome 1	100.18207	100.18215	100.18223	100.01920	100.01931	100.01944
Chromosome 2	100.24460	100.24462	100.24467	99.87137	99.87139	99.87142
Chromosome 3	100.07289	100.07292	100.07292	99.96253	99.96254	99.96255
Chromosome 4	100.04402	100.04405	100.04408	99.97075	99.97078	99.97078
Chromosome 5	100.25796	100.25797	100.25798	99.88001	99.88002	99.88003
Chromosome 6	99.96049	99.96052	99.96053	99.92795	99.92799	99.92801
Chromosome 7	100.13681	100.13684	100.13688	100.07917	100.07919	100.07922
Chromosome 8	99.88546	99.88549	99.88551	99.99190	99.99193	99.99197
Chromosome 9	99.94456	99.94466	99.94478	100.09470	100.09485	100.09498
Chromosome 10	100.11401	100.11407	100.11413	100.02763	100.02773	100.02780
Chromosome 11	100.02812	100.02813	100.02819	99.87830	99.87830	99.87832
Chromosome 12	100.07651	100.07656	100.07661	100.04336	100.04333	100.04333
Chromosome 13	100.26855	100.26860	100.26861	100.02271	100.02269	100.02270
Chromosome 14	100.80214	100.80216	100.80216	99.73124	99.73123	99.73124
Chromosome 15	99.88381	99.88387	99.88394	100.12357	100.12362	100.12368
Chromosome 16	100.56616	100.56621	100.56623	99.60341	99.60348	99.60352
Chromosome 17	100.21192	100.21197	100.21202	100.18038	100.18044	100.18049
Chromosome 18	100.10666	100.10667	100.10667	99.83600	99.83605	99.83606
Chromosome 19	100.27265	100.27268	100.27270	99.75734	99.75739	99.75739
Chromosome 20	100.22474	100.22477	100.22479	99.69416	99.69418	99.69423
Chromosome 21	99.32590	99.32591	99.32590	100.15602	100.15601	100.15602
Chromosome 22	99.40298	99.49307	99.49324	100.06869	100.06881	100.06887
Chromosome X	100.32044	100.32048	100.32052	99.89578	99.87581	99.87584
Chromosome Y	101.45477	101.45500	101.45514	99.53336	99.53400	99.53425
Whole genome	100.16515	100.16519	100.16522	99.94600	99.94604	99.94608

Table 9 – Verifying *Chargaff's* second parity rule at codon scale level in 24 individual human chromosomes.

Beyond Chargaff's second rule: *Do other kinds of symmetries exist?*

Analysing the “Codon Frequency Ratio” (CFR) in the Table 1 (at the top of the paper), we note strange pairs of correlations:

[TTT (2.4667) AAA (2.4566)], [TCT (1.4172) AGA (1.4144)], [CCC (0.8393) GGG (0.8403)], etc.

Here we classify populations of codons according to the universal genetic code table. Meanwhile, other kinds of classifications are possible. The simplest comes by sorting the 64 codon populations from most frequent to least frequent. (arranging in decreasing order of codon population frequencies).

Several chapters of the book *Codex Biogenesis* are dedicated to this topic (Perez, 2009). They elaborate on the discovery that for instance *across the 32 codon populations, the most frequent is exactly 2X as numerous as the least frequent of the 32 codons*. The exact ratio was 1.995859355.

They also prove that total atomic weights of each of the 2 simple DNA strands exhibit the same perfect symmetry: For the whole human genome, the balance ratio between both DNA strands is exactly = 1.000000456. Also, we noticed that this equilibrium has increased as the whole human genome sequence has grown in precision (successive releases of the draft human genomes sequences of April 2001, November 2002 and finally August 2003).

All these studies come from a "mosaic" human genome, a hybrid fusion of the genomes of numerous individuals. It is very likely that the specific genome from any individual would show even greater precision.

We also believe that telomeres and centromeres regions within chromosomes, which cannot be technologically sequenced, further contribute to optimize this already perfect balance.

Various other complementary symmetries and codon/nucleotide ratios are reported in the book *Codex Biogenesis* (Perez, 2009), demonstrating the evidence of other embedded levels of symmetry.

What kinds of symmetries?

Sorting codons in decreasing population frequency makes the phenomenon obvious: codons are ordered in pairs of similar frequency. The curve of figure d below shows this clearly.

What are the labels of these codon pairs? Why do they behave this way?

In Table 10, we sort codons by diminishing populations. The first line includes the first 2 codons of the 64. To the left the classified codon is first (TTT) and to the right the classified codon is second (AAA).

Their respective populations are very close and their CFRs (Codon Frequency Ratios) are almost identical. Finally, note that these 2 codons are complementary (AAA is the complementary codon of TTT using *Crick and Watson's* base pairing law).

Within this codon pairing scheme, we also see that the first 16 pairs (exactly half of the 64 codon labels) are very frequent (CFR > 1), while the 16 remaining pairs are least frequent (CFR < 1).

HUMAN GENOME "ARCHAIC CODE" Evidence

CODONS FREQUENCIES (cumulating the 3 codons reading frames)

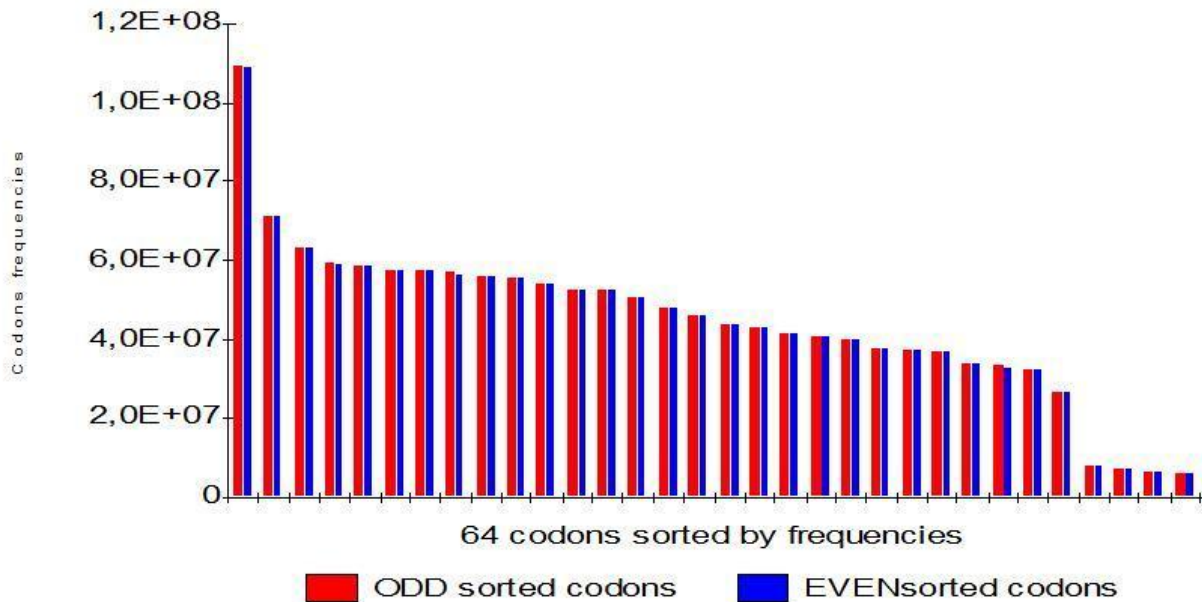


Figure d – Evidence of codon pairs when classifying codon populations by decreasing frequencies. This case adds the 3 codon reading frames; figure is from CODEX BIOGENESIS (Perez, 2009).

Odd classified codons				Even classified codons			
Codon Hits (odd)	Codon labels	Total Codon populations	"Codon Frequency Ratio" (CFR)	"Codon Frequency Ratio" (CFR)	Total Codon populations	Codon labels	Codon Hits (even)
1st	TTT	36530115	2.466678436	2.456629302	36381293	AAA	2nd
3rd	ATT	23669701	1.598285169	1.595875219	23634011	AAT	4th
5th	TCT	20990387	1.417365781	1.414570266	20948987	AGA	6th
7th	TTA	19750578	1.333648275	1.331661096	19721149	TAA	8th
9th	TAT	19568343	1.321342944	1.320017168	19548709	ATA	10th
11th	CTG	19195946	1.296197016	1.294913307	19176935	CAG	12th
13th	TGT	19152113	1.293237214	1.287907908	19073189	ACA	14th
15th	CTT	18944797	1.2792383	1.275856605	18894716	AAG	16th
17th	TTC	18708048	1.263251938	1.261228633	18678084	GAA	18th
19th	TCA	18565027	1.253594514	1.25339113	18562015	TGA	20th
.../...	TTG	18005020	1.215780311	1.210576601	17927956	CAA	.../...
	TGG	17480496	1.18036208	1.177941529	17444649	CCA	
	CAT	17423117	1.176487591	1.175538601	17409063	ATG	
	CCT	16835177	1.136787225	1.135140977	16810797	AGG	
	CTC	15942742	1.076525981	1.076301597	15939419	GAG	
31st	AGT	15266057	1.030833152	1.029847159	15251455	ACT	32nd
33rd	GGA	14619310	0.9871618724	0.986856594	14614789	TCC	34th
	GTG	14252868	0.9624180527	0.9598219375	14214421	CAC	
	GTT	13852086	0.935355441	0.9314501605	13794251	AAC	

	TGC	13649076	0.9216472884	0.9207256463	13635427	GCA	
	GCT	13252828	0.8948908329	0.8942085652	13242724	AGC	
	GAT	12658530	0.8547611465	0.8542053522	12650299	ATC	
	GGG	12446600	0.8404506752	0.8392612984	12428986	CCC	
	TAG	12240281	0.826519084	0.8249693963	12217331	CTA	
	GCC	11268094	0.7608726247	0.7601995403	11258126	GGC	
	GGT	11026602	0.7445659936	0.743263108	11007307	ACC	
.../...	GTA	10766854	0.7270266349	0.7262671867	10755607	TAC	.../...
55th	GTC	8955434	0.6047113712	0.6035903966	8938833	GAC	56th
57th	CCG	2606672	0.1760142724	0.1758509306	2604253	CGG	58th
59th	CGT	2379612	0.1606821551	0.1601840268	2372235	ACG	60th
61st	GCG	2247440	0.1517573044	0.1515541907	2244432	CGC	62nd
63rd	TCG	2087242	0.1409400116	0.1408038822	2085226	CGA	64th
	Total Odd ➔	474337193			473466674	← Total Even	

Table 10 – Reshaping Table 1 reveals evidence of codon pairs when sorting codon populations by decreasing frequency. “Odd” codons are codons classified 1 3 5...63 and “even” codons are codons classified 2 4 6... 64. Here we have restricted the analysis to the first codon reading frame single-stranded DNA sequence (data from Table 2).

Let us analyze the following pairs: ATT and AAT, then TCT and AGA, etc. There are strong correlations between populations, but even more remarkable is the following:

For any odd classified codon, the even classified codon faces its **mirror codon**. Specifically, every pair of codons is made up of a codon and its « mirror codon » or anticodon: If the codon is 5 '-ATG-3 ' then its anticodon will be 5 '-CAT-3 ' by the principle of base complementarity. This indicates a law which is borne out for the whole table. The 32 pairs of codons sorted by frequency are formed by a codon matched with its anticodon.

Consequence:

If the first *Chargaff* rule (double stranded DNA) seems natural, resulting from the law of *Crick-Watson* base-pair complementarity, then by the same token, the second *Chargaff* rule seems strange.

Why T=A and C=G within a single-stranded section of DNA?

We propose the following new rule:

In the whole human genome single-stranded DNA, the Chargaff's second parity rule is a consequence from another generic law:

The number of codons (i.e. TCG) = the number of anticodons (i.e. CGA).

The following hypothetical origin scenario involves this law:

Simple-stranded DNA results from an ancient ancestral double stranded DNA, particularly a hairpin-like DNA that might have been unfolded.

This would produce a single-stranded DNA where T=A and C=G as observed here.

Possible explanation: "Ancestral Genome" and Transposons.

We are confronted with an obvious perfect symmetry between the codons and their mirror-codons. We see odd/even pairs on the level of the whole human genome. In (Perez, 2009), we show that this law remains conserved regardless of individual genome SNP variability. We suggest that this discovery can be explained by an original double-stranded DNA which unfolded to produce a double-length mono-stranded DNA. DNA strand being unfolded like a "hairpin". This scenario could have been repeated multiple times, doubling the length of the genome each time. Then the primitive genome split up, giving rise to chromosomes. Multiple genome-wide rearrangements through transposition led to the current state of the human genome. Thus we have a parsimonious explanation for this strange symmetry of human genome codon frequencies. The reader will naturally ask: "*Why and how could this ancient code be preserved and maintained in spite of the changes and mutations during millions of years of evolution of the human genome?*"

In the 1940's and 1950's, Nobel prize winner *Barbara McClintock* discovered a peculiar phenomenon in maize: certain regions of a chromosome moved, or transposed, to other positions.

This was the discovery of TRANSPOSONS (Fedoroff, 1984): often called "jumping genes" because of their ability to "jump" to completely different regions within the chromosome and later "jump" back to their original positions.

Meanwhile, "jumping genes" is a misleading term because transpositions are related to noncoding areas as well as coding areas. A particular class of transposons moves from one place to another. (Class II transposons consist of DNA sections that move directly from place to place).

Sometimes there is a palindrome-like swap of the transposon during this move.

Example, the original sequence:

5' TAAGGCTATGC 3'
3' ATTCCGATACG 5'

... Moves to another genome region and becomes reversed as follows:

5' GCATAGCCTTA 3'
3' CGTATCGGAAT 5'

We found the same process here. It joins a codon with its "mirror-codon".

Perhaps DNA double strand topological reshaping processes could explain genesis of the reported facts (hairpin-like unfolding, Moebius-like ribbon, Class II transposons?)...

It seems that the genome regulates the behavior of transpositions according to the described rules of the « Golden Ratio Fractal Checksum Matrix ».

-4 - "Why is the Human Genome Codon Chaos Pattern not just Random or Chance?":

One might be tempted to ascribe the sequence of codons in DNA to "random chance". One could make the same judgment of cards in a poker game; certainly as you take cards off the stack, they appear to be random. However, we all know there is a very specific permutation structure in a complete set of 52 cards (spades, clubs, numbers, jacks, queens, kings, etc). As you remove certain cards from the stack, certain other cards necessarily remain. We have just shown here that the human genome is very similar to a card deck. In Table 10, about one billion codons are analogous to millions of 64-card poker games. To be more precise, they are games of 32 cards having equal likelihood of being "odd" or "even". There is another difference between codons and a card game: each of 32

cards has a different likelihood of chance, dictated by the CFR (codon Frequency Ratio) in Table 10. So even though the sequence of codons is superficially random, in reality this is not so. Rather, just as in a card game, the total composition of codon population obeys this explicit checksum structure, a «hidden order». There is a very definite «order within the chaos».

5 Speculations

Two questions remain unanswered:

Is the human genome sequence really fractal?

And why does it use the Golden Ratio in particular, since an infinite number of schemes are theoretically possible?

In (Perez, 1990), and (Perez, 1997), we presented strong mathematical relationships between Fractals and Golden ratio:

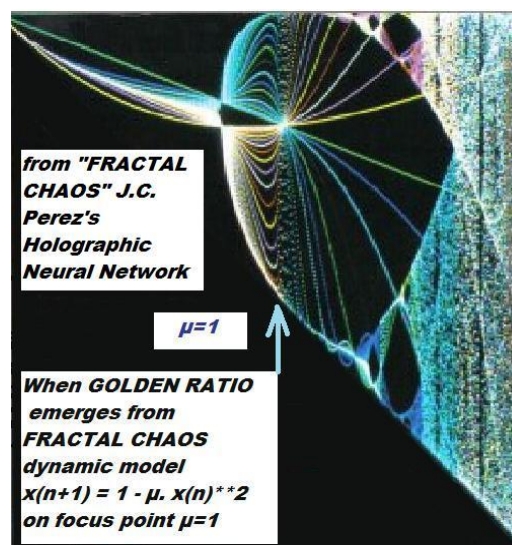


Figure e – Evidence of Golden ratio hypersensitivity in a specific region of the « Fractal Chaos » neural network model; Figure from (Perez, 1997).

We will answer these two questions in a future publication. Based on the numerical projection law of the C O N H bio-atoms average atomic weights below (figure f), we will reveal an integer number based code which unifies the 3 worlds of genetic information: DNA, RNA and amino acid sequences.

This code applied to the whole sequence of human genome, produces generalized discrete waveforms. We will show that, in the case of the whole double-stranded human genome DNA, the mappings of these waves fully correlate with the well known Karyotype spectral GIEMSA alternate dark/grey/light bands within chromosomes.

Then a very exciting question will emerge:

What hypothetical links exist between these theoretically predicted waveforms and the experimental electromagnetic waves detected by Luc Montagnier in HIV DNA (Montagnier et al., 2009)?

$$\text{Proj (m)} = [1 - [4\pi\sqrt{\varphi\varphi\varphi^2}]] m$$

with: $\sqrt{\varphi}=1/\sqrt{\Phi}$ *Phi is the GOLDEN RATIO* Φ
 $\varphi = 1 / \Phi$
 $\varphi^2 = 1/\Phi^2$

Figure f – A non linear projection formula provides a common whole number-based code unifying bio-atoms, nucleotides, codons, RNA, DNA and amino acids.

Acknowledgements: Many thanks to computer science book international author *Jacques de Schryver* and communications engineer & search engine specialist *Perry Marshall* (one of the world's leading specialists on WEB « *Google AdWords* ») for their precious help in English translation and discussions.

References

- [1] Affleck, I. 2010. Solid-state physics: Golden ratio seen in a magnet, *Nature* 464, 362-363.
- [2] Albrecht-Buehler, G. 2006. Asymptotically increasing compliance of genomes with Chargaff's second parity rules through inversions and inverted transpositions. *Proc Natl Acad Sci USA* 103, 17828-17833.
- [3] Baltimore, D. 2001. Our genome unveiled. *Nature* 409, 814-816.
- [4] Calleman, C. J., 2009. *The Purposeful Universe*, Bear § Co, Rochester USA, pp 153.
- [5] Coldea, R., et al. 2010. Quantum Criticality in an Ising Chain: Experimental Evidence for Emergent E8 Symmetry. *Science* 327, 177-180.
- [6] Euclid. 1533 first printed Edition. *Elements*. Book 6, Definition 3.
- [7] Fedoroff, N.V. 1984. Transposable genetic elements in maize. *Scientific American* 250, 84-98.
- [8] Gardner, M. 1967. *Mathematical Games*. *Scientific American* 216, 124-125. 118-120. and 217, 115.
- [9] Lander, E. 2009. *Science* 326, cover page.
- [10] Liebermann-Aiden, E., et al. 2009. Comprehensive mapping of long-range interactions reveals folding principles of the human genome *Exp. Science* 326, 289-293.
- [11] Mandelbrot, B.B. 1983. *The Fractal Geometry of Nature*, Freeman, New York.
- [12] Montagnier, L., et al. 2009. Electromagnetic detection of HIV DNA in the blood of AIDS patients treated by antiretroviral therapy. *Interdisciplinary Sciences: Computational Life Sciences* 1, 245-253.
- [13] Pellionisz, A. 2008. *The Principle of Recursive Genome Function*. *The Cerebellum*. Springer 7, 348-359.
- [14] Peng, C.K., et al., 1992. Long-range correlations in nucleotide sequences, *Nature* 356, 168-170.
- [15] Perez, J.C. 1990. Integers neural network systems (INNS) using resonance properties of a Fibonacci's chaotic golden neuron. *Neural Networks* 1, 859-865.
- [16] Perez, J.C. 1991. Chaos, DNA, and Neuro-computers: a golden link: the hidden language of genes, global language and order in the human genome. *Speculations in Science and Technology* 14, 336-346.

[17] Perez, J.C. 1994. Method for the functional optimization of high temperature superconductors by controlling the morphological proportions of their thin layers. (PCT/FR93/00782). International Européen PCT (Patent Cooperation Treaty) number WO94/03932.

[18] Perez, J.C. 1997. L'ADN décrypté, Resurgence, Liège Belgium.

[19] Perez, J.C. 2009. Codex Biogenesis, Resurgence, Liège Belgium.

[20] Rudner, R., Karkas, J.D., Chargaff, E. 1968. Separation of *B. subtilis* DNA into complementary strands. III. Direct Analysis. Proc Natl Acad Sci USA 60, 931-922.

[21] Yamagishi, M.E.B., Shimabukuro, A.I. 2008. Nucleotides frequencies in human genome and Fibonacci numbers. Bulletin of Mathematical Biology 70, 643-653.